Proceedings of ASME Turbo Expo 2011
GT2011
June 6-10, 2011, Vancouver, British Columbia, Canada

GT2011-45252

VALIDATION OF A FIRST VANE PLATFORM COOLING DESIGN

Joerg Krueckels, Will Colban, Michael Gritsch and Martin Schnieder

Alstom Power
Baden, Switzerland

ABSTRACT

Low emission requirements for large industrial gas turbines can be achieved with flat combustor temperature profiles reducing the combustor peak temperature. As a result the heat load on the first stage vane platforms increases and platform film cooling is an important requirement. Furthermore, high lift airfoils generate stronger secondary flows including complex vortex flows over the platforms, which impacts heat transfer coefficients and film cooling.

Cascade tests have been performed on a high lift profile with a platform film configuration and will be presented. The linear cascade was operated at engine representative Mach numbers. Pressure measurements are compared to design data to ensure correct operating conditions and periodicity of the cascade. The thermochromic liquid crystal measurement technique is used to obtain adiabatic film cooling effectiveness. The upstream gap (corresponding to the gap between the combustor and turbine) and the purge air exiting this gap are included in the investigations. The effect of the purge air on the recovery temperature is very strong and needs to be taken into account for the layout of the cooling scheme.

The heat transfer coefficient distribution on the platform is obtained for an uncooled configuration using a transient infrared imaging technique with heat flux reconstruction.

Computational fluid dynamics (CFD) assessments are used to support the validation results. Heat transfer coefficients and the effect of the purge air on adiabatic wall temperatures are compared with experimental results.

NOMENCLATURE

Symbols

AR	Film hole area ratio
Cax	Axial chord
C_p	Specific heat
C_1, C_2, C_3	Coefficients
D	Film hole diameter
h	Heat transfer coefficient
k	Thermal conductivity
M	Blowing ratio $(\rho_c u_c) / (\rho_g u_g)$
Ma	Mach Number
Nu	Nusselt Number = h cax / λ
q’’	Specific heat flux
P	Film hole pitch
t	Width of hole at break out
T	Temperature
x	Axial distance
X	Distance downstream of the film exit
λ	Thermal conductivity of air
ξ	Film-cooling scaling parameter
ρ	Density
τ	Data acquisition frequency
$\overline{\eta}$	Film effectiveness, lateral average

Subscripts

ad	Adiabatic wall
c	Coolant
g	Hot gas
m,n	Time step, index parameters
rec	Recovery

TLC	Thermo-Liquid Crystal
wall	Wall

INTRODUCTION

In order to achieve higher efficiencies in heavy-duty gas turbines, hot gas temperatures are increased while at the same time the cooling air consumption needs to be kept as low as possible. Additionally, low emission requirements are achieved with flat exit combustor temperature profiles. This increases the heat load on the first vane endwalls and requires an efficient and well-validated film cooling design. Linear cascade tests are an important part of the overall design and validation process, as explained in [1]. The present investigation shows how the film cooling scheme of a first vane platform is validated using cascade measurements and CFD.

The fundamental flow behavior in nozzle guide vane passages has been shown by Langston [2] and many others. The vortices and secondary flow movements strongly impact the heat transfer characteristics on the platforms. Blair [3] published one of the first works on endwall heat transfer coefficients and film cooling and found that both parameters are influenced by secondary flow. Friedrichs [4] investigated the distribution of film effectiveness produced by several rows of cylindrical holes on a vane endwall. In a subsequent study [5] he adapted the film-cooling layout according to the secondary flow patterns on the endwall. Since then, a lot of research has been done investigating the heat transfer and film effectiveness for film cooled vane platforms, as for example by Nicklas [6] and Knost [7] and many others. Barigozzi [8] and Colban [9] have compared fan-shaped with cylindrical cooling holes on vane endwalls and found a large improvement of the levels of film effectiveness. The importance of the upstream gap purge air on the platform adiabatic effectiveness has been shown by several publications, as for example Cardwell [10] and [11]. Despite the wide use in industry, there are only few publications about correlations for the film effectiveness of fan-shaped holes. A recent publication by Colban [15] explains the development of such a correlation covering a wide range of parameters. The correlation shown by Colban is based on flat plate data and does not take into account additional effects such as curvature and acceleration, which are relevant to blade and endwall configurations.

VALIDATION STRATEGY

In order to validate the platform film cooling design of a nozzle guide vane, cascade measurements of the film effectiveness including purge air and the heat transfer coefficients were performed in a linear cascade. With this, the thermal boundary conditions of the vane platform are obtained experimentally. CFD is an important building block in the validation approach, as it allows transferring the measurement results to engine conditions. First, a CFD calculation is performed modeling the cascade geometry and flow parameters. Experimental results are compared in detail with obtained predictions and deviations are recorded in terms of enhancement factors. A second CFD simulation is then done for the engine conditions including geometrical details not present in the cascade. Major geometrical differences between cascade and engine are the fillets at the transition from airfoil to endwall and the converging annulus. Then, the enhancement factors found in the first comparison are applied to the CFD results at engine conditions and provide an improved prediction of the thermal boundary conditions of the vane in the engine. This provides accurate boundary conditions for the mechanical model, which allow then a reliable lifetime prediction. Special focus must be given to the thermal boundary conditions of the endwalls and fillets, as typically the life limiting areas for low cycle fatigue are in these regions. An approach for obtaining cyclic life is outlined in [12].

HIGH SPEED LINEAR CASCADE

The in-house high-speed linear cascade is described in [13]. A high-lift nozzle guide vane, as previously described in [14], was investigated. In contrast to the previously reported investigations, the focus of the current study is the film effectiveness and heat transfer coefficient distributions on the endwalls, meaning that some modifications were required. The cascade featured 3 vane passages at engine scale. The height of the wind tunnel was 150mm and the vane-to-vane pitch was 210 mm. The airfoil geometry was derived from a mid-span profile of a typical first stage vane of a power generation gas turbine.

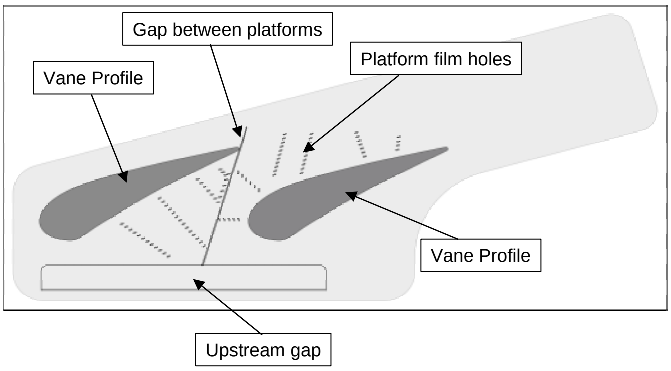

Figure 1: Test model of the vane platform used for the measurement of film effectiveness in the linear cascade

Two two-stage radial compressors provided the main air ("hot gas"). The compressors are designed to provide a maximum of 11 kg/s of air at a pressure of 1.6 bar to the wind tunnel. For this specific vane setup with three passages, the compressors delivered approximately 6.2 kg/s air to the wind tunnel, at a total pressure of about 1.1 bar. Before entering the test section the air was heated by means of a 600kW electrical heater, which operated in both a steady-state (film effectiveness) and transient (heat transfer coefficients) mode.

The air then passed through a set of flow conditioners and entered the test section (Figure 2) through an inlet nozzle, accelerating the flow up to $Ma_{inlet}=0.16$, resulting in an inlet Reynolds number of roughly 8 x 10^5 based on axial chord. A turbulence intensity level of 5% at the vane leading edge was achieved by means of a turbulence grid that was located approximately one and a half chord lengths upstream of the leading edge. Adjustable tailboards controlled the flow distribution between the three passages. Downstream of the test section the flow was decelerated through a diffuser section before being exhausted into the atmosphere through a silencer.

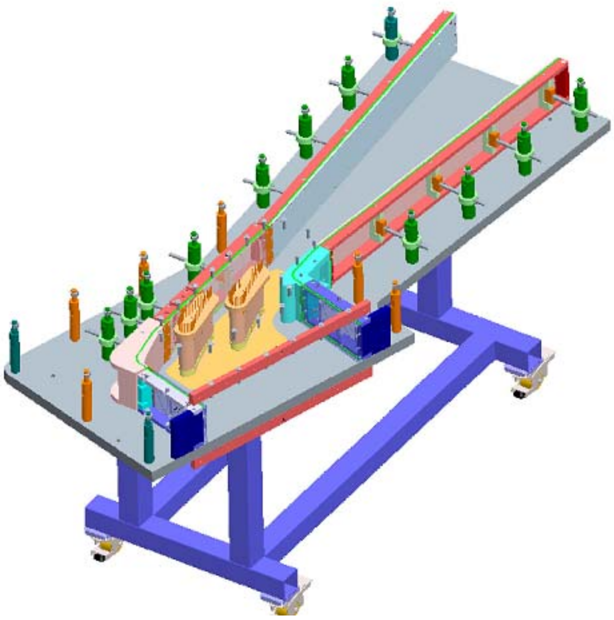

Figure 2: Linear vane cascade rig

For the measurements of film effectiveness and purge air distribution, carbon dioxide (CO_2) was used to simulate the coolant. The CO_2 was taken from a pressurized 10 m^3 liquid-CO_2 storage tank and passed through a vaporizer before entering the vane cascade. The use of CO_2 as coolant resulted in density ratios between the coolant and the main air that are close to real engine conditions. The coolant was supplied to several plenums located below the vane platform and then fed to the individual rows of film cooling holes. The coolant flows were individually controlled for each plenum by needle valves and measured by means of flow meters.

MEASUREMENT TECHNIQUE

To measure the film effectiveness the vane platform was coated with narrow-banded thermo-liquid crystals (color change at 42°C, band width 1°C), which were used as an indicator of the platform surface temperature distribution during testing (Figure 3). Only the hues values corresponding to the green color, which represent the highest intensity, were used for the post-processing. Pictures of the entire platform surface were taken using three miniature CCD cameras. Optical access was provided by means of Perspex windows located in the top wall of the wind tunnel. The pictures were then transformed spatially in order to accurately represent the true surface distance. Prior to testing, a 5mm x 5mm grid was placed on the platform surface and reference pictures were taken at each viewing location and used to perform a spatial transformation for each TLC picture. The hue values at each pixel in the transformed pictures were then converted into temperatures by means of a calibration that was done as a pre-test. The coolant total pressures were measured in the coolant plenums inside the vane platform. The local main gas recovery temperature distribution was derived from a pre-test carried out without coolant injection. Knowing these quantities a distribution of the local film cooling effectiveness could be computed, using the following equation.

$$\eta = \frac{T_{rec} - T_{TLC}}{T_{rec} - T_c}$$

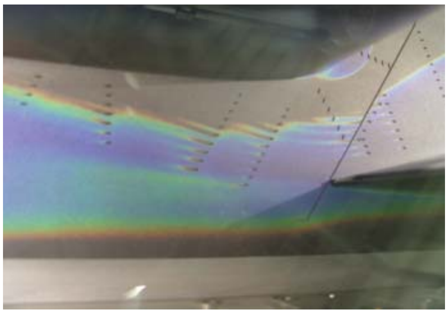

Figure 3: Platform for measurement of the film cooling effectiveness instrumented with TLC in the cascade

For a given operating condition, the narrow-banded TLCs provided only a limited surface coverage (Fig. 3). Therefore, a special procedure was applied in order to achieve full coverage of the entire vane platform surface. Pictures were taken at different hot gas temperature (T_g) levels, from roughly 75°C down to 40°C. Changing T_g shifted the TLC line to different positions across the surface. In total, 30-40 individual images were obtained for each test case, which were then analyzed to yield film effectiveness on the platform. The first step for each camera view was to transform the images into the global 2D coordinate system(Fig. 4). Then, the individual pictures were linked and merged into one global 2D contour plot for each test case.

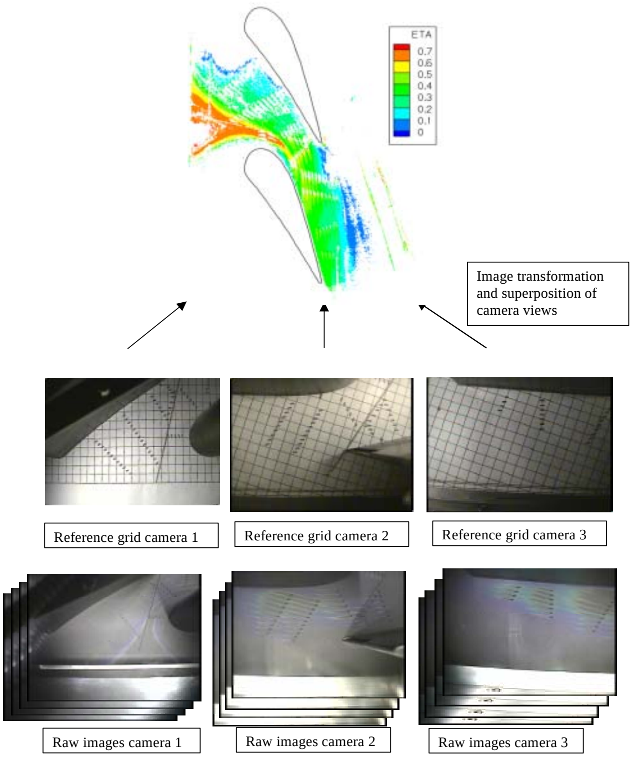

Figure 4: Process for combining raw images into a contour plot of film effectiveness

Experiments were carried out at three different blowing ratios representing a nominal flow case (M @ 100%), a high flow case (M @ 120%), and a low flow case (M @ 80%) in order to determine the sensitivity of film cooling performance with respect to variations of the coolant flow rate.

For the measurement of the heat transfer coefficients, a transient infrared (IR) technique was used, similar to the one described by O'Dowd et al. [19]. This method involved bringing the cascade to a steady-state condition at a low temperature (roughly 30°C), and then increasing the hot gas temperature in a transient manner. The hot gas temperature history—which did not resemble a step-change, but rather like an asymptotic change due to the thermal inertia of the system—was recorded using thermocouples located at the cascade inlet, while the surface temperature history on the vane platform was recorded using an IR camera (FLIR model SC3000, thermal sensitivity of 0.03K @ 30°C). The recorded surface temperature history was then used to compute the instantaneous local heat flux, according to the method derived by Oldfield et al. [20],

$$q''(t) = q''(m\tau) = 2\sqrt{\left(\frac{\rho c_p k}{\pi\tau}\right)}\sum_{n=0}^{m}\left[\sqrt{m-n}\left(T_{n-1} - 2T_n + T_{n+1}\right)\right]$$

Prior to the transient tests, an in-situ, low-speed (to negate aerodynamic heating effects), linear (valid assumption for small range of interest), pixelwise calibration was performed for the IR images using thermocouples on the platform surface and the cascade inlet. The local recovery temperature distribution was derived from a steady-state IR image taken prior to the transient test at the same flow conditions. At this point, it is possible to plot a series of points for each pixel corresponding to ($T_{rec}(t) - T_{wall}(t)$) versus q"(t). The heat transfer coefficient is then simply the slope of the linear curve fit, with origin at 0, as shown by the example in Figure 5. Four different mainstream heater voltage settings, which dictated the rate of hot gas temperature increase, were used for each image location. The data shown in Figure 5 represent the first few seconds of the transient temperature increase.

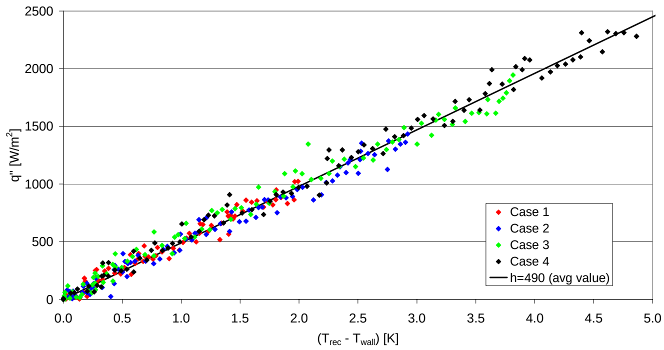

Figure 5: Example of method for determination of heat transfer coefficients

Six camera positions were required to cover the entire platform surface (Figure 6). At each location, the image sequences were first calibrated and then spatially transformed using reference pins located on the surface. Then, the series of images were converted into heat transfer coefficients and combined with the images taken at the other locations to produce the final result covering the entire vane platform surface.

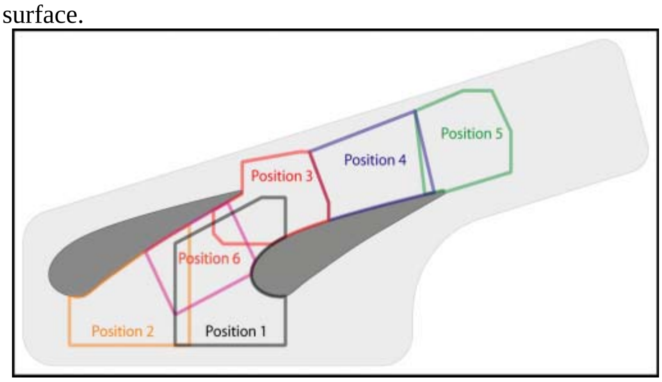

Figure 6: Image locations for heat transfer measurements

The partial derivative method given by Moffat [16] was used to calculate uncertainties for the measured values. The uncertainties for the adiabatic effectiveness measurements were 2% for high values of $\eta > 0.7$ and 6.8% for a low value of $\eta = 0.2$. The uncertainties for the heat transfer coefficient measurements ranged from 5.2% at low values (Nu=950) to 8.1% at high values (Nu=2700).

The measurement of the heat transfer coefficients was done without the upstream gap and without any film cooling holes. Measurements of the heat transfer coefficients with film cooling will be done as a next step.

VANE AND FILM COOLING SCHEME

A high lift profile suitable for a first vane of a heavy-duty gas turbine is the subject of investigation. 11 rows of fan-shaped film cooling holes are distributed over the platform as shown in Figure 1. As the split line between adjacent vane platforms influences the flow field and has an impact on the cooling films, it was also modeled in the cascade, however without the injection of leakage air.

To check the cascade flow conditions, measurements of static pressure around the airfoil at midspan were taken and compared against predictions. The comparison is shown in Figure 7.

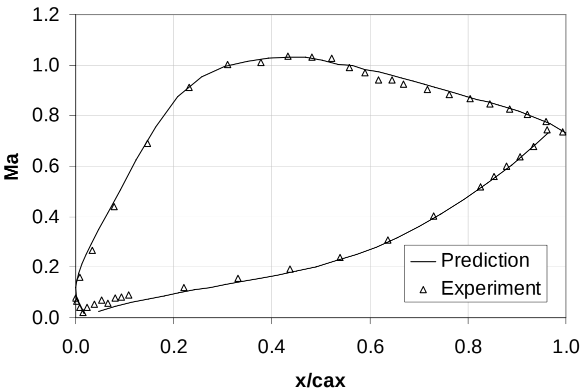

Figure 7: Isentropic Mach number comparison for the high-speed linear cascade

In order to gain an insight into the secondary flow patterns on the platform surface, oil flow streak lines were recorded for the vane endwall and are shown in Figure 9. The separation line of the horseshoe and passage vortices from the endwall is visible, and so is the secondary flow towards the suction side at mid-passage.

NUMERICAL APPROACH

A hybrid mesh for the cascade was created using CENTAUR. As stated above, the measurement of film effectiveness was done with the upstream gap between combustor and first vane present. For this case, a mesh was generated with 6.3 million cells. On the vane platform, y+ varies between 0.5 near the inlet and 3 in the areas of high velocities. Computations were done with FLUENT V6.3.26 using the realizable k-ε turbulence model.

Figure 10 shows surface streaklines on the vane platform from the simulation, superimposed on the oilflow picture obtained in the cascade. The patterns showing the separation line and the secondary flow are similar to the ones obtained in the cascade, however the location of the saddle point is predicted closer to the leading edge. The inlet boundary layer of the cascade was not measured. The expected boundary layer thickness at the inlet of the CFD domain was set according to a correlation.

In the experimental setup for obtaining the heat transfer coefficients, the upstream gap was not present in order to simplify the measurements. For this case, an unstructured hybrid mesh was used with 5.1 million cells and a y+ less than 1 at the platform walls to ensure good resolution of the boundary layer. Therefore, no wall functions were used. Grid independence tests have been done earlier on similar geometries but not specifically for this case. The results have been transferred to this case. A fine mesh was generated with a strong clustering of cells around the airfoil and the endwall in order to capture well the vortices. A mesh detail of the leading edge area with platform is shown in Figure 8.

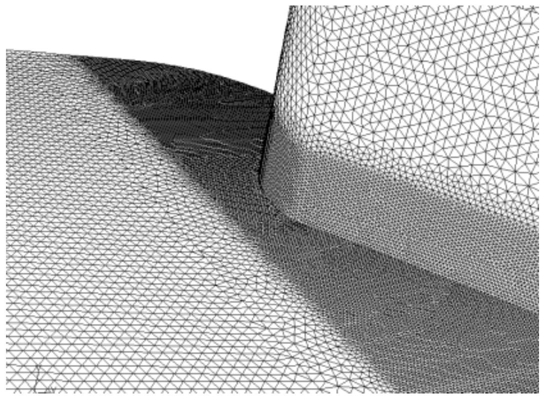

Figure 8 - Mesh detail at the airfoil / endwall intersection

In order to calculate the heat transfer coefficient, first an adiabatic calculation was performed to get the recovery temperature at the walls. Then the wall temperature was specified at a level realistic for the cascade and the distribution of the heat fluxes at the walls obtained. The heat transfer coefficient was then calculated by combining both calculations with

$$h = \frac{\dot{q}}{\left(T_{ad} - T_{wall}\right)}$$

The prediction of the heat transfer coefficients was done for both the realizable k-ε and the v2f turbulence models.

Figure 9: Oilflow streak lines on the vane endwall surface

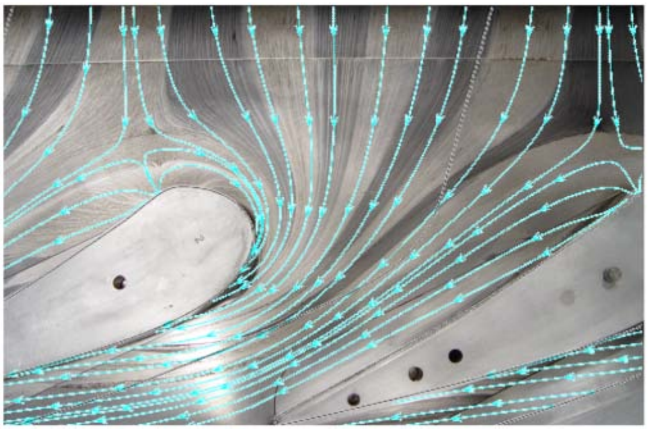

Figure 10: Surface streaklines - CFD result superimposed on oilflow streaklines

APPROACH FOR PREDICTING FILM EFFECTIVENESS

The ability of steady Reynolds averaged Navier-Stokes predictions with turbulence models to predict film effectiveness is limited. They are not able to predict the correct amount of mixing between coolant film and hot gas. A better match can be obtained with unsteady DES or LES computations and has been shown for simple geometries. However, for design applications with a large number of cooling holes, the computational effort for DES and LES is too high. Therefore, a different approach using experimental correlations is used. From the CFD result, streamlines in a layer close to the endwall representative of the film injection are extracted. Along these streamlines, the recently published correlation for fan-shaped holes [15] is applied, whenever the streamline crosses a film row. The correlation has the following form:

$$\overline{\eta} = \frac{1}{P/t + C_1 M^{C_2} \xi^{C_3}}$$

The film cooling scaling parameter is defined as:

$$\xi = \frac{4}{\pi} \frac{\frac{X}{D} \frac{P}{D}}{M \cdot AR}$$

The superposition approach from Sellers [21] is used, if subsequent film rows are crossed. The film effectiveness on the streamline points in 2D are then triangulated to provide a contour plot.

RESULTS – FILM EFFECTIVENESS

The experimental film effectiveness, including purge flow from the upstream gap, is shown in Figure 11. What is important is, that in the area downstream of the aerodynamic throat the film traces show less secondary flow than one would expect from the oil flow traces in Figure 9.

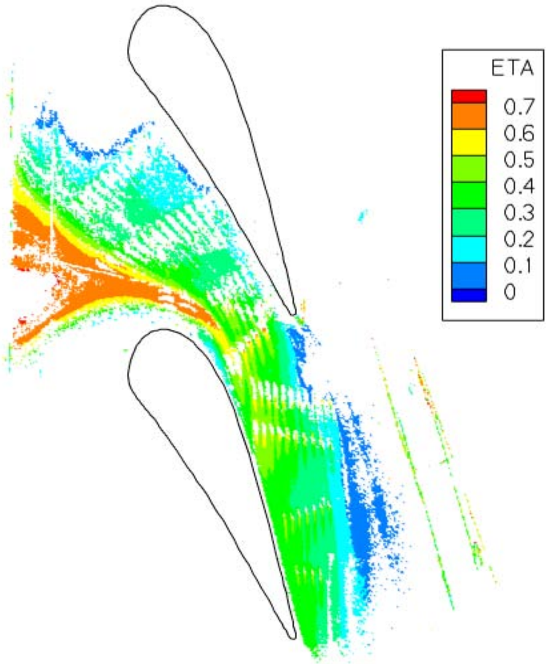

Figure 11: Film effectiveness at nominal blowing rate including gap purge air

Figure 12 shows the comparison of measured film effectiveness at the nominal blowing rate, compared to the prediction using the correlation approach outlined above. For this comparison, the experimental result without gap purge is used as the correlation approach does not provide results for the purge air film effectiveness. Figure 12 shows streamlines, along which the laterally averaged film effectiveness was extracted for the experimental data and is compared to the correlation approach in Figure 14.

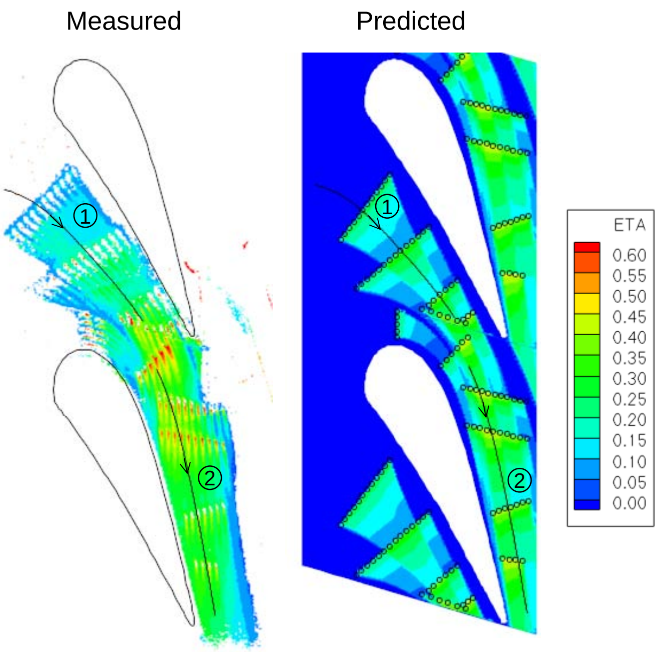

Figure 12: Measured film effectiveness (left) compared with prediction (right) at nominal blowing rate, streamlines for comparison

Along streamline 1, upstream of the aerodynamic throat, the correlation approach predicts too high levels of film effectiveness close to the film injection. At streamline 2, downstream of the throat, the match is quite good for the last three film rows. Note that the correlation used is quite simple and was built using flat plate data. For a better match, in-house correlations taking into account effects of the local velocity field and acceleration are used.

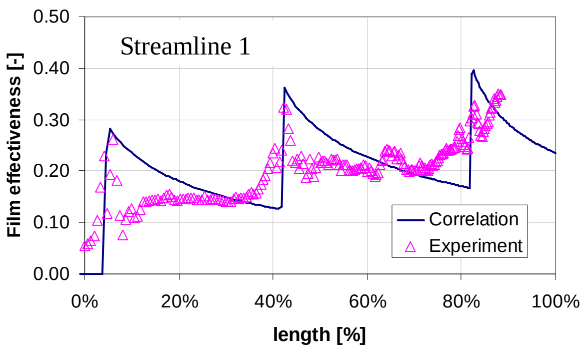

Figure 13: Comparison between correlation approach and laterally averaged experimental data along streamline 1

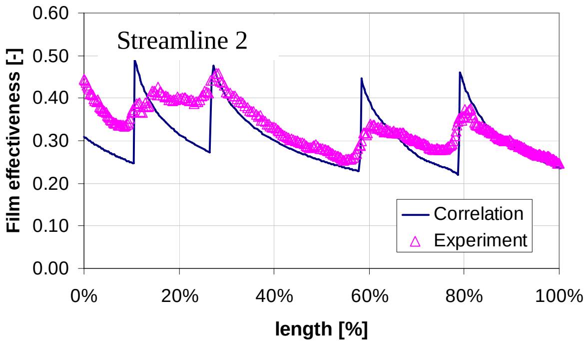

Figure 14: Comparison between correlation approach and laterally averaged experimental data along streamline 2

CFD allows a better understanding of the flow phenomena at the gap between combustor and turbine, which is modeled in the cascade for the measurements of film effectiveness. The main flow features are highlighted in Figure 15. Upstream of the vane, high pressure drives some of the main flow into the gap where it mixes with the purge air. In the area of low pressure near the suction side, the flow leaves the gap and creates an area with high film effectiveness on the platform.

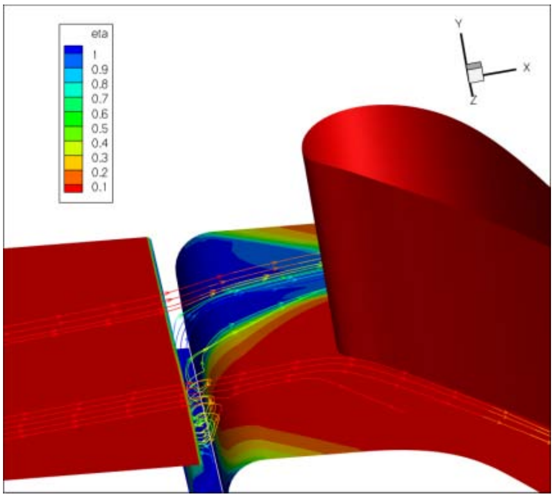

Figure 15: Main gas flow interaction with purge air - surface contours and streamlines colored with mixing effectiveness

The predicted film effectiveness is compared with measured data in Figure 16. Please note that the TLC method is not able to detect film effectiveness near zero, therefore, no data is supplied in those regions. The location of the purge air path over the platform is well predicted, however the level of film effectiveness is far too high. The steady RANS calculation using the realizable k-ε turbulence model is not able to predict the mixing between hot gas and purge air correctly.

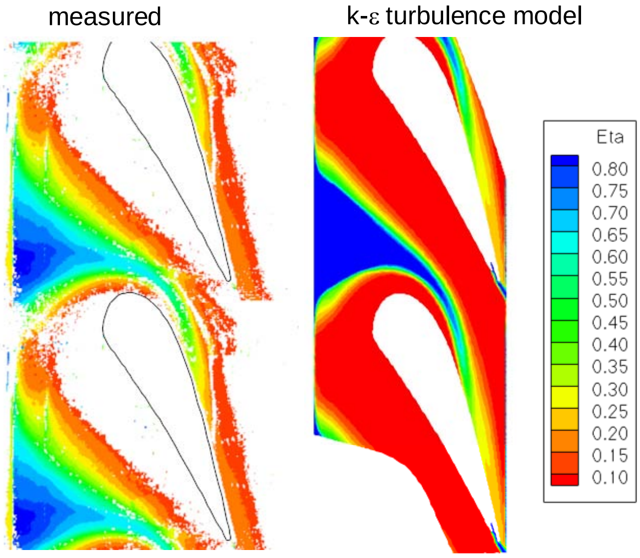

Figure 16: Measured (left) and predicted / k-ε (right) film effectiveness due to gap purge

RESULTS – HEAT TRANSFER COEFFICIENT

For comparing measured Nusselt number with prediction, computations with two different turbulence models were done. Previous investigations have indicated a better performance of the v2f turbulence model for assessing endwall heat transfer coefficients [18]. Figure 17 compares the experimental results with predictions. The overall levels of Nusselt number are predicted well. Measurements show areas of high Nu at the suction side shoulder of the airfoil and on the pressure side approaching the trailing edge. CFD captures this effect but the area of high Nu is smaller and the peak level is not reached.

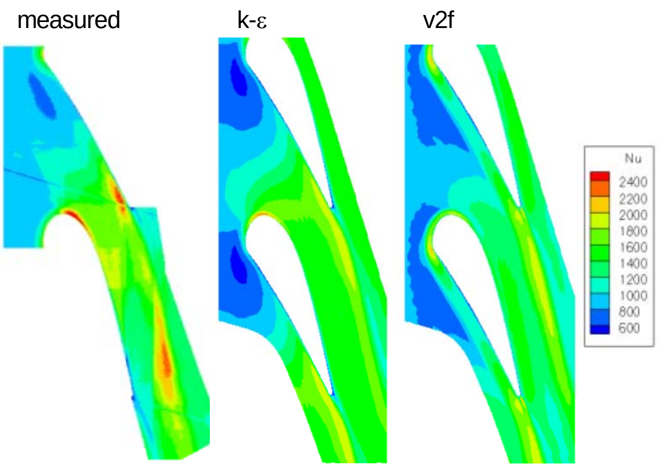

Figure 17: Measured Nusselt number (left) compared to CFD results using realizable k-eps (middle) and v2f model (right)

In order to perform a more detailed comparison, three lines of constant axial coordinate were chosen as shown in Figure 18. Experimental and predicted Nusselt numbers are compared along these lines in Figure 19, Figure 20 and Figure 21. The previously found superiority of the v2f model cannot be confirmed. Instead, the computationally less expensive realizable k-epsilon model agrees better with measurements and performs quite well in predicting the Nusselt number on the vane platform. The peak levels at x/cax = 50% near the suction side and at x/cax = 90% near the pressure side are not fully reached. Only the v2f model shows the vortex area along the pressure side boundary to the airfoil, which creates an area of higher Nu numbers. This area of higher Nu is not confirmed by the experiment and is not predicted by the realizable k-ε model.

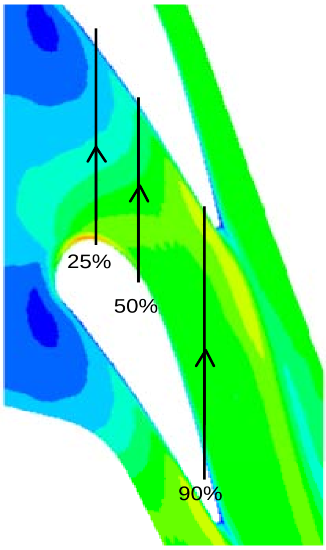

Figure 18: Lines (axial positions) for detailed comparison of Nusselt number

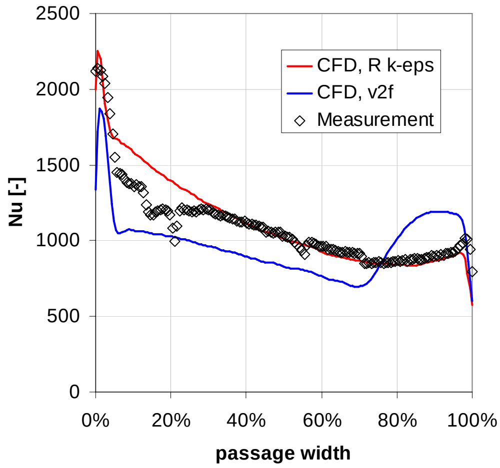

Figure 19: Nusselt number comparison at x/cax = 25 %

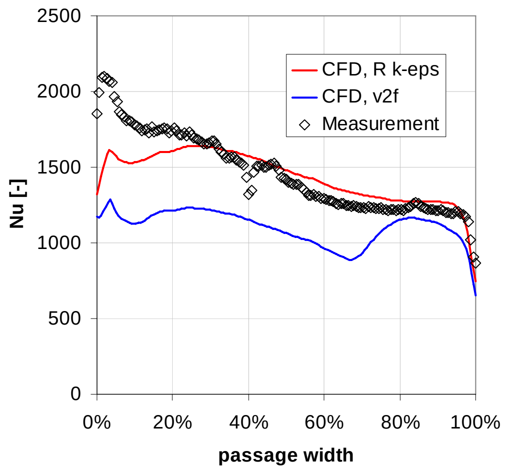

Figure 20: Nusselt number comparison at x/cax = 50 %

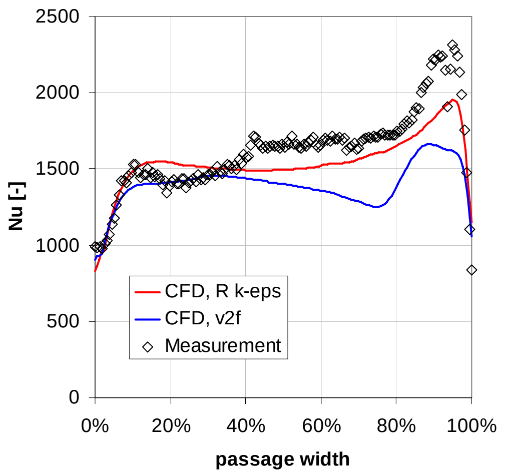

Figure 21: Nusselt number comparison at x/cax = 90 %

In order to understand the reason for the high levels of Nusselt number near the SS shoulder of the airfoil and near the PS trailing edge, the flow features in the CFD simulation were investigated. No strong vortex flow could be detected in these areas. Both points are close to the aerodynamic throat, where highest velocities occur. Therefore, these areas are adjacent to the areas of high Nusselt number on the airfoil, as shown in Figure 22 and Figure 23. This finding shows that it is mainly a 2D flow effect due to the high velocity and acceleration.

CONCLUSIONS

In today's advanced heavy-duty gas turbines the heat load on the first vane platforms is increasing, therefore an accurate knowledge of the thermal parameters (film cooling effectiveness and heat transfer coefficient) is key for a successful design. In order to obtain these parameters, measurements in a high-speed linear cascade were done. The film effectiveness produced by several rows of fan-shaped holes including purge air was measured using thermochromic liquid crystals. The heat transfer coefficients were obtained using a transient infrared imaging technique.

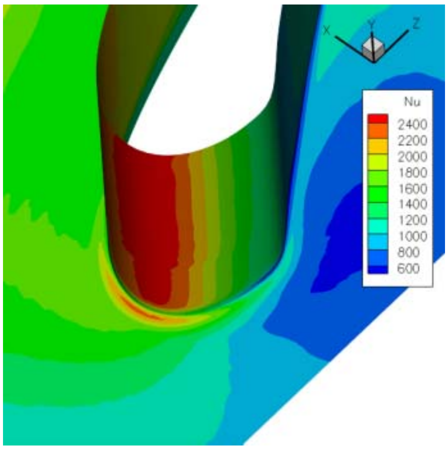

Figure 22: Area of high Nu near the SS shoulder corresponds to high Nu on the airfoil

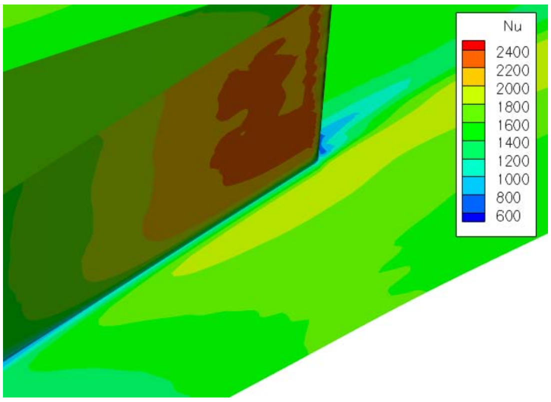

Figure 23: Area of high Nu number near the PS trailing edge on the platform with corresponding area on the airfoil

The measured film effectiveness corresponds to a certain degree with a correlation for fan-shaped holes applied to streamlines covering the platform. Using more elaborate correlations, this approach has the potential for an improved prediction of vane end wall film effectiveness.

CFD is able to correctly predict the location of the purge air streak over the platform from the upstream gap. However, the level of film effectiveness is over predicted.

Comparison between predicted and measured Nusselt number shows a good agreement. The realizable k-ε turbulence model performs well in predicting endwall Nusselt numbers.

The experimental data is used to validate and improve design tools, which then allow an accurate prediction of the component temperatures at engine conditions. This study is an important step in validating the cooling design for first stage platforms at high heat load.

REFERENCES

[1] Krueckels, J., Arzel, T., Kingston, T. R., Schnieder, M., 2007, "Turbine Blade Thermal Design Process Enhancements for Increased Firing Temperatures and Reduced Coolant Flow," ASME Paper GT2007-27457.

[2] Langston, L. S., 2001, "Secondary Flows in Turbines – A Review," Annals of the New York Academy of Sciences, Vol. 934, Issue Heat Transfer in Gas Turbine Systems, pp. 11-26.

[3] M. F. Blair, 1974, "An experimental study of heat transfer and film cooling on Large-Scale Turbine Endwalls," ASME Journal of Heat Transfer, Vol. 96, pp. 524.529.

[4] Friedrichs, S., Hodsin, H. P., Daws, W. N., 1996, "Distribution of Film-Cooling Effectiveness on a Turbine Endwall Measured Using the Ammonia and Diazo Technique," ASME Journal of Turbomachinery, 1996, Vol. 118, pp. 613-621.

[5] Friedrichs, S., Hodson, H. P., Dawes, W. N., 1996, "Design of an improved endwall film-cooling configuration," ASME Journal of Turbomachinery, 121, pp. 772-780.

[6] Nicklas, M., 2001, "Film-cooled turbine endwall in a transonic flow field: Part II – heat transfer and film cooling effectiveness," ASME Journal of Turbomachinery, 123, pp. 720-729.

[7] Knost, D. G., Thole, K. A., 2005, "Adiabatic Effectiveness Measurements of Endwall Film-Cooling for a First Stage Vane," ASME Journal of Turbomachinery, Vol. 127, pp. 297-305.

[8] Barigozzi, G., Benzoni, G., Franchini, G., Perdichizzi, A., 2006, "Fan-Shaped Hole Effects on the Aero-Thermal Performance of a Film Cooled Endwall," ASME Journal of Turbomachinery, Vol. 128, pp. 43-52.

[9] Colban, W., Thole, K. A., Haendler, M., 2008, "A comparison of Cylindrical and Fan-Shaped Film-Cooling Holes on a Vane Endwall at Low and High Freestream Turbulence Levels," ASME Journal of Turbomachinery, Vol. 130, pp. 031007-1-9.

[10] Cardwell, N. D., Sundaram, N., Thole, K. A., 2006, "Effect of Mid-Passage Gap, Endwall Misalignment and Roughness on Endwall Film-Cooling" ASME Journal of Turbomachinery, Vol. 128, pp. 62-70.

[11] Cardwell, N. D., Sundaram, N., Thole, K. A., 2007, "The Effects of Varying The Combustor-Turbine Gap," ASME Journal of Turbomachinery, Vol. 129, pp. 756-764.

[12] Muecke, R., Woratat, P., 2009, "A Cyclic Life Prediction Approach for Directionally Solidified Nickel Superalloys," ASME GT2009-59180.

[13] Krueckels, J., Gritsch, M., Schnieder, 2009, "Design Considerations and Validation of Trailing Edge Pressure Side Bleed Cooling", ASME GT2009-59161.

[14] Stephan, B., Krueckels, J., Gritsch, M., 2010, "Investigation of Aerodynamic Losses and Film Cooling Effectiveness for a NGV Profile," GT2010-22810.

[15] Colban, W. F., Thole, K. A., Bogard, D., 2011, "A Film-Cooling Correlation for Shaped Holes on a Flat-Plate Surface," ASME Journal of Turbomachinery, January 2011, Vol. 133.

[16] Moffat, R.J. 1988, "Describing the Uncertainties in Experimental Results," Experimental Thermal and Fluid Science, Vol. 1, pp. 3-17.

[17] Shih, T.-H., Liou, W. W., Shabbir, A., Yang, Z., and Zhu, J., 1995 "A New - Eddy-Viscosity Model for High Reynolds Number Turbulent Flows - Model Development and Validation." Computers Fluids, 24(3). 1995, :227-238

[18] Hermanson, K., Kern, S., Picker, G., Parneix, S., 2003, "Predictions of External Heat Transfer for Turbine Vanes and Blades With Secondary Flowfields," ASME Journal of Turbomachinery, Vol. 125, pp. 107-112.

[19] O'Dowd, D., Zhang, Q., Ligrani, P., He, L., and Friedrichs, S., 2009, "Comparison of Heat Transfer Measurement Techniques on a Transonic Turbine Blade Tip," ASME Paper No. GT2009-59376.

[20] Oldfield, M. L. G., Jones, T. V., and Schultz, D. L., 1978, "On-Line Computer for Transient Cascade Instrumentation," *IEEE Transactions on Aerospace and Electronic Systems*, Vol. AES-14, no. 5, pp. 738-749.

[21] Sellers, J. P., 1963, "Gaseous Film Cooling with Multiple Injection Stations," *AIAA Journal*, Vol. 1, pp. 2154-2156.